**Summary:** Three complementary techniques that probe different characteristics of curing: FTIR microspectroscopy, confocal microscopy and axisymmetric adhesion testing were used to study discrete epoxy samples cured at different temperatures and to follow curing across a continuous gradient combinatorial library. Together, these techniques provide a comprehensive picture of chemical and physical changes.

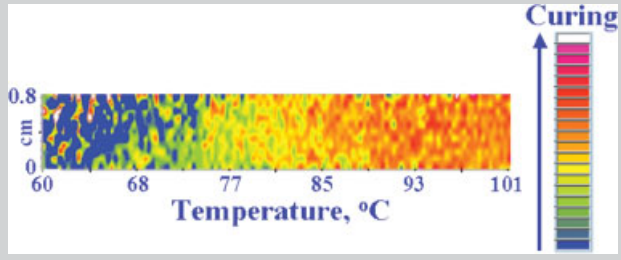


FTIR microspectroscopy map of epoxy film cured on a temperature gradient. Red represents the highest and blue the lowest curing.

# Combinatorial Approach to Characterizing Epoxy Curing

*Naomi Eidelman,*[1] *Dharmaraj Raghavan,*[2] *Aaron M. Forster,*[3] *Eric J. Amis,*[3] *Alamgir Karim*[3]

[1] American Dental Association Foundation – Paffenbarger Research Center, National Institute of Standards and Technology, 100 Bureau Drive Stop 8546, Gaithersburg, MD 20899-8546, USA[a]
Fax: (301) 963-9143; E-mail: naomi.eidelman@nist.gov
[2] Department of Chemistry, Howard University, Washington DC 20059, USA
E-mail: draghavan@howard.edu
[3] Polymers Division, National Institute of Standards and Technology, Gaithersburg, MD 20899, USA

Received: October 9, 2003; Revised: October 31, 2003; Accepted: November 5, 2003; DOI: 10.1002/marc.200300190

**Keywords:** adhesion; confocal microscopy; curing; epoxy; FTIR microspectroscopy

## Introduction

Thermoset resins are an important class of engineering polymers that account for nearly 20% of the polymers market, which encompasses composites, adhesives and coatings.[1] Currently quality control of cured thermoset resins is accomplished through off-line, destructive mechanical testing of finished parts or online monitoring of curing by less intrusive techniques such as near-infrared[2] or fluorescence spectroscopy.[3] Variations in starting materials (e.g. resin type and lot), curing conditions (e.g. time and temperature) and storage conditions result in large variability in the degree of curing and a substantial scrap rate for high volume manufacturing processes involving fast curing cycles.[3]

An essential component of intelligent manufacturing is a test method that can quickly assess the extent of resin curing (ultimately on-line) and adjust the processing conditions to obtain a cured resin of reproducible quality. The span of process parameter space (time, temperature, composition) and the complex interaction between these variables pose a challenge for investigation by conventional experimental techniques, which often rely on manipulating a single parameter over several experiments. Combinatorial and high throughput (CHT) methods provide the rapid, systematic generation of experimental data over multi-parameter spaces. Accordingly, CHT methods represent an efficient route for screening resin batches to determine the optimum parameters required for a target curing protocol. The CHT techniques for sample characterization need to be non-destructive and time efficient. Consequently, combinatorial approaches to materials science require the development of flexible techniques that work in unison to produce a complete picture of mechanical,[4] kinetic[5,6] or adhesive[7–9] processes.

In this study, three complementary high-throughput techniques: Fourier transform-infrared microspectroscopy in reflectance mode (FTIR-RM), confocal microscopy and Johnson, Kendall, and Roberts (JKR) adhesion tests were

[a] Official contribution of the National Institute of Standards and Technology; not subject to copyright in the United States.

 DOI: 10.1002/marc.200300190 

used to measure the effect of temperature on the curing process of discrete epoxy films and to map the properties of a film cured on a temperature gradient stage for a short time. FTIR-RM was used to monitor the epoxide ring absorption (916 $cm^{-1}$) within several μm of the epoxy surface. Confocal microscopy was used to measure the emission fluorescence intensity maximum from 505 nm to 550 nm of a fluorophore embedded within the epoxy film. Finally, adhesion measurements were employed to measure the work of debonding (WOD) at the epoxy-air interface during curing.

FTIR spectroscopy has previously been used to follow the epoxide ring disappearance (curing kinetics) of individual epoxy films at various temperatures.[9–11] Transmission FTIR microspectroscopy has been applied previously to cross-sections of bilayers of epoxy blends.[12] FTIR-RM mapping is a non-contact, non-destructive method for characterizing surface chemical composition both qualitatively and quantitatively. It has been used previously to determine the distribution of different chemical components in human gallstones,[13] the mineral and collagen in dentin,[14] and the mineral and resins in dental composites[15] but was used for the first time in this study to map the curing of epoxy films.

Confocal microscopy was used to monitor epoxy curing because of its depth selectivity and non-destructive nature. During curing there is a significant change in the epoxy microviscosity which can be gauged by doping the resin with an appropriate fluorophore molecule. The restricted fluorophore mobility increases the emission intensity because the fluorophore can dissipate the excitation through non-radiative processes less effectively. While fluorescence has been used to study the curing characteristics of bulk epoxy resin and silanized glass/epoxy interfaces,[3,16–19] confocal microscopy has not been used to map a temperature gradient cured epoxy library at or near the surface of the film.

The JKR test[20] geometry was used to monitor adhesive properties at the epoxy surface during curing. This axisymmetric test employs a single elastomeric lens that is compressed against (loading) and then removed from (unloading) a flat substrate while measuring load and contact area. The mechanical and chemical changes that occur during epoxy curing strongly affect interfacial adhesive properties. The work of debonding (WOD) discussed here concerns the total energy required to remove the lens from the epoxy film at room temperature.

## Experimental Part

A stock solution of 0.52 mg of fluorescent dye (4-dimethylamino-4′-nitrostilbene) in 4.01 g of curing agent (2,4,6-tri(dimethyl amino methyl)phenol) was prepared and stirred for two days. A batch of stock solution was prepared to facilitate the creation of both discrete and gradient films to ensure the dye concentration was constant within each film. Immediately before creating the epoxy films, the stock solution was diluted with diglycidyl ether bisphenol A epoxy resin (DGEBA) and an additional amount of curing agent to obtain 10 wt.-% of curing agent. Epoxy films were prepared by flow coating the epoxy mixture onto clean glass substrates.[21] In flow coating, a cylindrical bar is dragged across a bead of uncured resin to create a film of uniform thickness. The discrete films were heated for 1 h at distinct temperatures (25 to 90 °C) in a convection oven (±1 °C) and were tested with all three techniques at random $x$, $y$ locations. Additionally, an epoxy film (≈400 μm thick) was placed on a temperature gradient stage[21] to cure for 15 min. The temperature stage exposes the epoxy film to a linear temperature gradient from 55 to 102 °C (±1 °C). The gradient film was mapped first by FTIR-RM, followed by the fluorescence and adhesion techniques at the same positions.

### *FTIR Microspectroscopy (FTIR-RM)*

The FTIR-RM analyses were performed using a Nicolet Magna-IR 550 FTIR spectrophotometer interfaced with a Nic-Plan IR microscope operated in reflectance mode. The microscope is equipped with a video camera, a liquid nitrogen-cooled mercury cadmium telluride (MCT) detector (Nicolet Instrumentations Inc. Madison, WI, USA) and a computer-controlled translation stage (Spectra-Tech, Inc., Shelton, CT, USA), programmable in the $x$ and $y$ directions. Three spectra were collected from each discrete film in the 650 $cm^{-1}$ to 4 000 $cm^{-1}$ region with 8 $cm^{-1}$ resolution, 256 scans and a beam spot size of 300 μm × 300 μm. The spectral point-by-point mapping of the surface of the gradient cured epoxy film was performed in a grid pattern with the use of the computer-controlled microscope stage and Atlus mapping software. Since the surface of the film was not perfectly smooth and its thickness was not uniform (due to viscosity changes during gradient curing), care was taken to mount the sample such that a major portion of the film was in approximately the same focal plane. First, the film was mapped with large steps (11 points spaced 5 mm apart along the center line ($x$ axis) of the film following the temperature gradient and 11 points 4 mm above and below the center line, giving a total of 33 lattice points) with manual focusing on each spot before a spectrum with 256 scans was collected.[14] The spectra extracted from this map were used for quantitative analysis of the extent of curing. The set of locations (relative to the edges of the glass substrate) from which spectra were collected defined a virtual grid used to template subsequent fluorescence and adhesion measurements. Second, the film was mapped automatically. Spectra were collected every 400 μm along the $x$ axis and 800 μm along the $y$ axis (a total of 1 386 spectra) with 64 scans per acquired spectrum. The spectra of both maps were collected in the 650 $cm^{-1}$ to 4 000 $cm^{-1}$ region with 8 $cm^{-1}$ resolution and an aperture of 400 μm × 400 μm. The reflectance spectra were proportioned against a background of a gold-coated disk and transformed to absorbance spectra using the Kramers-Kronig transform algorithm[22,23] for dispersion correction. The FTIR-RM maps were processed as ratios of the areas under the 916 $cm^{-1}$ epoxide ring peak and the 830 $cm^{-1}$ constant peak (used as an internal standard) of the 1-4 substituted aromatic

 

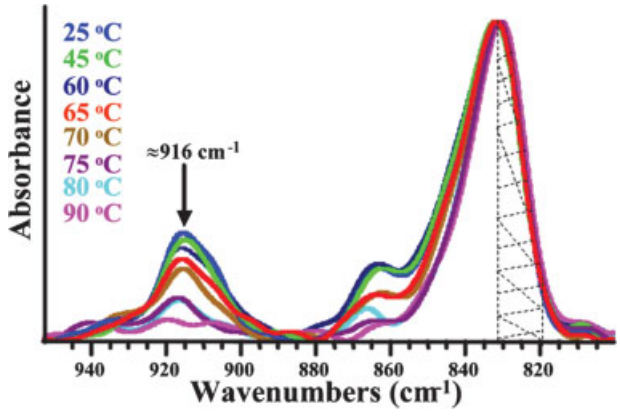


Figure 1. FTIR spectra of discrete films cured at various temperatures (the hatched region represents the area under the 830 $cm^{-1}$ peak that served as an internal standard).

rings in the DGEBA molecule and displayed as color contour maps. Extracted spectra from the manually focused map were baseline corrected between 953 $cm^{-1}$ and 800 $cm^{-1}$. The areas under the 916 $cm^{-1}$ ($A_{916}$) and 830 $cm^{-1}$ ($A_{830}$) peaks were measured and their ratios serve as a relative measure of curing degree ($CD = A_{916}/A_{830}$). A lower *CD* value is indicative of higher curing. Note that the constant partial area of the 830 $cm^{-1}$ peak (Figure 1) was used for $A_{830}$ because only this segment does not change during the curing process.

### *Confocal Microscopy*

The curing of epoxy films was monitored using an upright laser scanning confocal microscope (Zeiss LSM 510). The key feature of the LSM is that only light from a narrow objective focal plane is detected. The fluorescence doped epoxy films were excited at 488 nm using $Ar^+$ laser light and light emitted (505 nm to 550 nm) from the sample was detected with a photomultiplier tube. The 20× objective used gave a 512 μm × 512 μm field of view and a focal plane resolution depth of 5 μm. Images and fluorescence intensity data were acquired by focusing the laser beam near or just beneath the surface of the films. Images and intensity values at each location along the virtual grid of the gradient cured film were obtained using a computer controlled positioning stage. The image acquisition time was 30 s per position. The discrete images were regrouped according to the FTIR-RM defined virtual grid to reconstruct the surface fluorescence map.

### *Adhesion Measurements*

Hemispherical polydimethylsiloxane (PDMS) lenses were created by placing small drops of Dow Sylgard 184 (15:1 ratio of prepolymer to catalyst) onto a fluorinated glass slide.[24] The lenses were cured at 75 °C for 1 h in a convection oven, extracted in toluene over several days and dried under vacuum for 24 h. The calculated radius of curvature, determined from contact angle measurements, ranged between 1.0 mm and 3.5 mm for all lenses. The JKR adhesion testing geometry is described in detail elsewhere.[25] The PDMS lens is fixed to a small glass slide using only lens-glass adhesive contact and mounted to a 50 g load cell in line with a piezoelectric actuator to provide controlled positioning. A fiber optic displacement sensor measures lens displacement throughout the test and the contact area is imaged via a Leica DMIRE inverted microscope. The lens was brought within a few micrometers of the surface, displaced (towards the specimen) by a total distance of 25 μm at a velocity of 200 $nm \cdot s^{-1}$ and then completely removed from the epoxy at the same speed with no set dwell time. A tack curve was generated from the maximum lens displacement ($\delta_{max}$) to lens detachment ($\delta_0$) and the WOD was calculated according to Equation (1):[26]

$$\mathrm{WOD} = \int_{\delta_0}^{\delta_{max}} P\mathrm{d}\delta \Big/ \pi a_{max}^2 \qquad (1)$$

where $P$ is the load, $\delta$ is the displacement and $a_{max}$ is the maximum contact radius. Normalization to the maximum contact area permits a comparison of different samples and test areas along the gradient sample. The largest $a_{max}/h$, where $h$ is the lens height, was 0.4. On occasion, surface defects prevented adhesion testing in the positions of the FTIR-RM defined virtual grid. In these cases, testing was performed as close as possible to the pre-defined coordinates.

## Results and Discussion

Initially, the discrete sample measurements (cured at different temperatures for 1 h) are discussed, in order to demonstrate the ability of the techniques to track changes in the epoxy film during curing. The base-line corrected FTIR spectra of eight discrete films in the 800 $cm^{-1}$ to 953 $cm^{-1}$ spectral region are shown in Figure 1. The peak at 916 $cm^{-1}$, which is associated with the epoxide ring absorbance of the DGEBA molecule,[9,11] decreases monotonically with increasing curing temperature. The gradual decrease of this peak reflects the reaction of epoxide rings to form ether linkages. The *CD* (FTIR-RM) and fluorescent intensity values obtained from the discrete films are presented as a function of increasing curing temperature in Figure 2. A distinct break in the *CD* and in the fluorescence intensity was detected near a curing temperature of 60 °C. As the fluorescence intensity is nearly a mirror image of the epoxide ring absorption (FTIR-RM), the two techniques correlate with each other fairly well. A comparison of fluorescence intensity and *CD* values of films cured for 1 h at 90 °C and at 25 °C shows a five-fold increase in the fluorescence intensity and a five-fold decrease in the *CD*. Although there are no reports of fluorescence data at or near the surface of thin epoxy films, it is known from a previous study[16] that a seven to ten-fold increase in fluorescence intensity is expected upon curing bulk epoxy resin. This increase in fluorescence intensity is interpreted as a measure of degree of curing in polymer systems.[27] Since the local fluorophore environment (polymer network architecture, instrumentation factors, oxygen content, etc.)

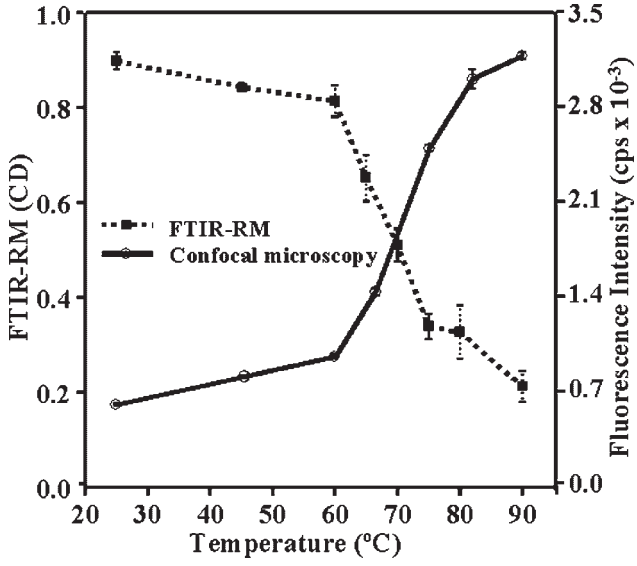


Figure 2. Averages and standard deviations of the *CD* (FTIR-RM) and of the fluorescence intensity of discrete films as a function of increasing curing temperature (error bars represent the experimental uncertainty at each temperature).

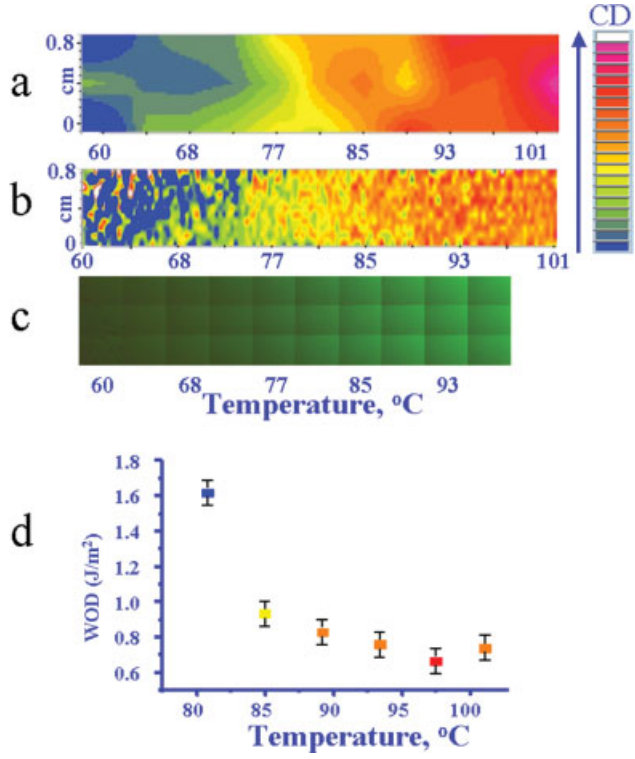


Figure 3. a) FTIR map (5 mm × 4 mm steps); b) FTIR map (400 μm × 800 μm steps); c) Fluorescence map; and d) WOD graph of the 15 min temperature gradient cured film (error bars represent the instrument uncertainty).

influences the fluorescence intensity,[16] generally IR or rheological measurements are used to verify the extent of curing in bulk epoxy resin systems. Figure 2 demonstrates the ability of confocal microscopy and FTIR-RM techniques to follow the changes in epoxy films subjected to different curing temperatures. The WOD was measured on discrete films only above 80 °C because these films were irreversibly deformed below this temperature. The WOD values at 80 and 90 °C were not significantly different.

The FTIR contour maps of the epoxy film, cured on the temperature gradient stage for 15 min, are shown in Figure 3a and 3b. The colors are a qualitative representation of the curing degree. Red represents the highest curing, and blue represents the lowest curing. A gradient in the colors from blue on the left (lowest temperature) to red on the right (highest temperature) is seen in both maps. The corresponding florescence map is shown in Figure 3c. Lighter green represents higher fluorescence intensity (higher degree of curing), which is indicative of a more established epoxy network at the higher curing temperatures. Conversely, darker green represents a lower degree of curing at lower temperatures. A strong gradient in the fluorescence intensity from 75 to 97 °C is observed, while below 75 °C the fluorescence intensity changes are less noticeable. The fluorescence measurements were discontinued at temperatures above 97 °C.

Adhesion measurements taken along the center line of the film are shown in Figure 3d. WOD reproducibility was established through previous measurements above and below the center line (results not shown). Due to the viscous nature of the epoxy film at low curing temperatures, measurements were discontinued at 80 °C, the point at which the epoxy surface was irreversibly deformed (as determined from optical microscopy). A two-fold decrease in the WOD, from 1.62 $J \cdot m^{-2}$ to 0.83 $J \cdot m^{-2}$ ($\pm 0.07$ $J \cdot m^{-2}$), is observed from 80 to 90 °C. The sharp drop in WOD may result from the conversion of mobile chains at the surface. These chains would provide a source of dissipation that requires additional energy to drive crack propagation.[28–32] The monotonic decrease in WOD above 85 °C may be a result of the further conversion of epoxy groups to ether groups at the surface[33,34] but further analysis is required to confirm this hypothesis.

The *CD*, fluorescence intensity and the WOD results of the gradient film are plotted as a function of the curing temperatures in Figure 4. A qualitative correlation between the three techniques across the temperature gradient is clearly seen. Note also that the three techniques had a similar spot size and penetration depth (measured at or within a few microns of the surface). Comparing the FTIR results of the 90 °C, 1 h cured discrete film ($0.212 \pm 0.033$) to the similar temperature results (89 °C) on the gradient film ($0.537 \pm 0.011$) indicates that the epoxy was not fully cured after 15 min curing. The simultaneous effects of gradient temperature and time on epoxy curing are the subjects of future study.

 

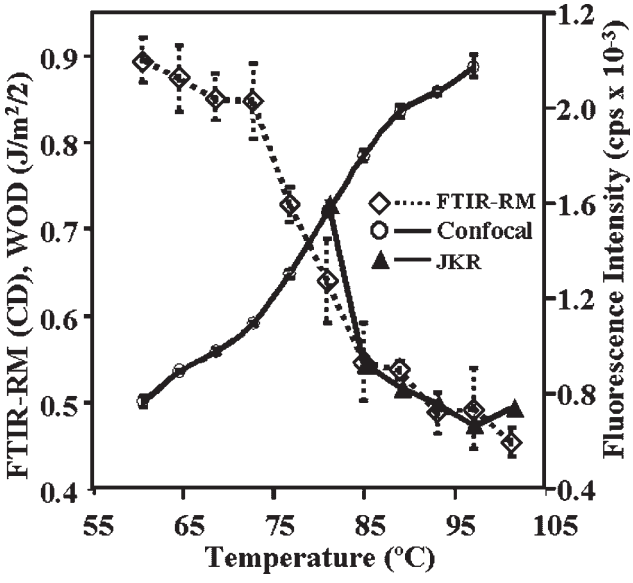


Figure 4. *CD*, fluorescence intensity and WOD across the 15 min temperature gradient cured film. The *CD* and fluorescence intensity data points represent the averages of the three measurements along the *y* axis at each temperature (error bars represent the standard deviations at each temperature).

## Conclusions

We have demonstrated a high-throughput approach to map, compare and correlate complementary chemical, physical and adhesive properties of an epoxy resin library undergoing curing by three independent methods: FTIR-RM, confocal microscopy and JKR adhesion tests. As expected, the FTIR-RM and fluorescence intensity measurements on discrete and gradient cured films show that the decrease in epoxide ring absorbance occurs parallel to the increase in fluorescence intensity. The decrease in WOD correlates with the epoxide ring disappearance above 80 °C. Future work will focus on the correlation of these techniques throughout the full curing cycle and quantification of the infrared, fluorescence and adhesion measurements to the state of epoxy curing.

## Disclaimer

Certain commercial materials and equipment are identified for adequate definition of the experimental procedures. In no instance does such identification imply recommendation or endorsement by NIST that the material or the equipment is necessarily the best available for the purpose.

*Acknowledgement:* This study was supported in part by *NIST Combinatorial Methods Center* and by *ADAF*. D. Raghavan was on a sabbatical from *Howard University* during the investigation.

[1] J. R. Fried, "*Polymer Science and Technology*", Prentice Hall Press, NJ 1995, p. 4.
[2] J. P. Dunkers, K. M. Flynn, R. S. Parnas, *Compos. Part A, Appl. S.* **1997**, *28A*, 163.
[3] D. L. Woerdeman, J. K. Spoere, K. M. Flynn, R. S. Parnas, *Polym. Compos.* **1997**, *18*, 133.
[4] K. L. Beers, J. F. Douglas, E. J. Amis, A. Karim, *Langmuir* **2003**, *19*, 3935.
[5] A. P. Smith, J. F. Douglas, J. C. Meredith, E. J. Amis, A. Karim, *Phys. Rev. Lett.* **2001**, *87*, 8701.
[6] R. A. Potyrailo, B. J. Chisholm, D. R. Olsen, M. J. Brennan, C. A. Molaison, *Anal. Chem.* **2002**, *74*, 5105.
[7] R. A. Potyrailo, R. J. Wroczynski, J. P. Lemmon, W. P. Flanagan, O. P. Siclovan, *J. Comb. Chem.* **2003**, *5*, 8.
[8] R. A. Potyrailo, B. J. Chisholm, W. G. Morris, J. N. Cawse, W. P. Flanagan, L. Hassib, C. A. Molaison, K. Ezbiansky, G. Medford, H. Reitz, *J. Comb. Chem.* **2003**, *5*, 472.
[9] T. M. Don, J. P. Bell, *J. Appl. Polym. Sci.* **1998**, *69*, 2395.
[10] F. Barbadillo, R. Losada, M. Suarez, J. L. Mier, L. Garcia, S. Naya, *Mater. Sci. Forum* **2003**, *426–432*, 2163.
[11] J. M. Barton, I. Hamerton, B. J. Howlin, J. R. Jones, S. Y. Liu, *Polym. Bull. (Berlin)* **1994**, *33*, 347.
[12] C. Spiteri, M. F. Vallat, J. Schultz, A. Belgrine, G. Evrard, A. Coupard, *Vide: Sci., Tech. Appl.* **1994**, *272*, 470.
[13] E. Wentrup-Berne, L. Rintoul, J. L. Smith, P. M. Fredericks, *Appl. Spectrosc.* **1995**, *49*, 1028.
[14] W. Tesch, N. Eidelman, P. Roschger, F. Goldenberg, K. Klaushofer, P. Fratzl, *Calcif. Tissue Int.* **2001**, *69*, 147.
[15] D. Skrtic, J. M. Antonucci, E. D. Eanes, N. Eidelman, *Biomaterials* **2004**, *25*, 1141.
[16] J. L. Lenhart, J. H. Van Zanten, J. P. Dunkers, R. S. Parnas, *Macromolecules* **2001**, *34*, 2225.
[17] W. Dang, N. H. Sung, *Polym. Eng. Sci.* **1994**, *34*, 709.
[18] B. Strehmel, V. Strehmel, M. Younes, *J. Polym. Sci., Part B: Polym. Phys.* **1999**, *37*, 1367.
[19] S. D. Schwab, R. L. Levy, *Adv. Chem. Ser.* **1990**, *227*, 397.
[20] K. L. Johnson, K. Kendall, A. D. Roberts, *Proc. R. Soc. London, Ser. A* **1971**, *324*, 301.
[21] J. C. Meredith, A. P. Smith, A. Karim, E. J. Amis, *Macromolecules* **2000**, *33*, 9747.
[22] J. M. Chalmers, N. J. Everall, S. Ellison, *Micron* **1996**, *27*, 315.
[23] J. A. Reffner, W. T. Wihlborg, *Am. Lab.* **1990**, *22*, 26.
[24] M. K. Chaudhury, M. J. Owen, *Langmuir* **1993**, *97*, 5722.
[25] A. J. Crosby, A. Karim, E. J. Amis, *J. Polym. Sci., Part B: Polym. Phys.* **2003**, *41*, 883.
[26] A. J. Crosby, K. R. Shull, *J. Polym. Sci., Part B: Polym. Phys.* **1999**, *37*, 3455.
[27] R. Vatanparast, S. Y. Li, K. Hakala, H. Lemmetyinen, *Macromolecules* **2000**, *33*, 438.
[28] F. Lapique, K. Redford, *Int. J. Adhes. Adhes.* **2002**, *22*, 337.
[29] F. D. J. Chu, R. E. Robertson, *J. Adhes.* **1995**, *53*, 149.
[30] P. J. Pearce, B. C. Ennis, I. Grabovac, C. E. M. Morris, *J. Adhes.* **1994**, *47*, 123.
[31] D. L. Woerdeman, N. Amouroux, V. Ponsinet, G. Jandeau, H. Hervet, L. Leger, *Compos. Part A, Appl. S.* **1999**, *30*, 95.
[32] M. Deruelle, H. Hervet, G. Jandeau, L. Leger, *J. Adhes. Sci. Technol.* **1998**, *12*, 225.
[33] D. Ahn, K. R. Shull, *Langmuir* **1998**, *14*, 3646.
[34] S. Kim, G. Y. Choi, A. Ulman, C. Fleischer, *Langmuir* **1997**, *13*, 6850.